CODE 27

A COMPREHENSIVE APPROACH TO THE PERFORMANCE-BASED DESIGN OF FAÇADE SOLUTIONS AGAINST RAINWATER PENETRATION

ABSTRACT

Rainwater penetration into building façades causes several issues, including material and structural weakening, reduction of their energy efficiency and negative health effects on occupants. Currently, the watertightness of building envelopes is characterised by international testing approaches, which recreate water supplies and pressure differences that do not represent the range of exposure combinations that can occur at each façade location and configuration. As a result, the choice of suitable façade systems for each situation has a qualitative and imprecise nature, leading to poorly optimised designs. This work expounds a comprehensive approach for the performance-based design of actual façades against rainwater penetration anywhere. For this purpose, it is determined the recurrence with which will occur, for each façade to be designed, the exposures tolerated by the façade solution during any watertighness test. This recurrence, characterised as a return period, defines the façade performance at its final operating conditions and depends on the exposure tested (the greater its magnitude and duration, the greater the severity and associate return period), on the site climatic conditions, and on the façade configuration (height and surroundings). The universal and quantitative nature of this design verification procedure is illustrated with examples of different building façades in two Spanish cities (Pontevedra and Málaga), within the framework of the HUEFAES research project (PID PID2021-122203OB-I00).

KEYWORDS: Wind-driven rain; Building façades; Rainwater penetration; Performance-based design; Return period.

1. INTRODUCTION

Rainwater penetration causes multiple issues related to the thermal performance of the building façades, premature deterioration of construction materials, and health concerns for occupants of the buildings (such as asthma and respiratory symptoms) [1-3]. Precipitation diverted by wind action, known as wind-driven rain (WDR), is the main source of water on building façades [3]. In conjunction with simultaneous wind pressure (driving rain wind pressure or DRWP), both contribute to rainwater runoff exceed the thresholds of surface tension and capillary pressure of water existing in the pores of the construction materials, thus causing rainwater infiltration [4-5].

Over the years, multiple studies have characterised WDR exposure of building façades in many regions, mainly using semi-empirical approaches based on the so-called ‘WDR relationship’ [6-7]. Occasionally, the analysis of simultaneous DRWP has complemented the previous characterisation [8-9].

However, in practice, practitioners base their design decision on the performance of façade configurations during standardised watertightness tests in which, for economic and functional reasons, the WDR and DRWP exposures expected on each case study are not recreated. Instead, the façade samples are subjected to a constant water supply and incremental pressure differences, whose generic values vary in each international test [10-11]. Given that these test parameters are not related to the extreme exposures expected in each situation, the façade performance against rainwater penetration remains unknown. Thus, neither the traditional WDR and DRWP studies can support performance-based designs, nor are current façade designs based on anything other than a purely qualitative approach.

To address this issue, a correlation between standardised exposure parameters used in testing and actual exposures of any façade was proposed (Bayesian performance-based method or BPB method) [12]. To achive this, the return period at which the combination of tested parameters would occur at any specific façade defined by its location, height and surroundings, was calculated. The method was extended to consider the influence of the different exposure durations recreated in watertightness tests in the calculation of the return period [13], to include more accurate estimates of the wind profile under unstable atmospheric conditions, and to correct the WDR value associated with the predominant raindrop diameter [14]. This work illustrates the use of the BPB method in façade designs in two Spanish cities, while also addressing in a comprehensive and functional manner some methodological challenges that are still present in the BPB method and affect its applicability and reliability.

2. BACKGROUND OF THE BPB METHOD.

On the basis of the performance demonstrated by each façade configuration during the watertightness test (water spraying and maximum pressure difference withstood without water leakage), the BPB method determines the recurrence at which WDR and DRWP exposures equivalent to those maxima surpassed during the trial will occur [12-14]. This recurrence, characterised as a return period, quantifies the façade performance at its final operating conditions and depends on the site climatic conditions, on the façade features (height and surroundings), and on the recreated exposure that has been withstood (the greater its magnitude and duration, the greater the severity and associated return period).

Firstly, the DRWP exposure on the façade is estimated by using the Bernoulli equation (Eq. 1), where $DRWP_z$ (Pa) represents the driving rain wind pressure at the façade height z (m) and z_o (m) is the roughness length of surrounding terrain, whose value is tabulated in the literature [15]. This roughness length is considered in the Hellmann friction coefficient of the wind profile power-law by means of an empirical formula suitable for unstable atmospheric conditions [16-17], such as those linked to the WDR events. U_{10} (m/s) expresses the wind speed records concurrent with rainfall, usually collected in open area and at a height of 10 m above ground level (2 m for agroclimatic weather data). For a conservative estimation, a pressure coefficient $C_p = 1$, a constant air density $\rho = 1.2$ kg/m^3 and a wind direction perpendicular to the façade orientation ($\cos\theta = 1$) are considered, thus simplifying Eq. 1.

$$DRWP_z \approx C_p \cdot \frac{1}{2} \cdot \rho \cdot \left(U_{10}\right)^2 \cdot \left(\frac{z}{10}\right)^{2\cdot\left[0.18+0.13\cdot\log z_0+0.03\cdot\left(\log z_0\right)^2\right]} \cdot \cos\theta \tag{1}$$

Secondly, the WDR exposure is determined in Eq. 2 by combining a corrected semi-empirical WDR relationship [18-19], a driving rain factor based on the inverse of the terminal falling speed of raindrops [18], and an estimate of the predominant spherical diameter of those droplets calculated from rainfall records R_h (l/m^2) [20]. Thus, WDR_z (l/m^2) represents the amount of wind-driven rain collected at the façade height z (m), while U_{10} (m/s) indicates the simultaneous wind speed, considering the adjustments already mentioned in Eq. 1. To provide a conservative estimate for the most unfavourable area, a rain admittance factor RAF = 0.9 can be considered for the uppermost corners of the building façade.

$$WDR_Z \approx 1.14 \cdot RAF \cdot \frac{U_{10} \cdot \left(\frac{z}{10}\right)^{\left[0.18+0.13\cdot\log z_0+0.03\cdot\left(\log z_0\right)^2\right]}}{-0.16603\cdot\left(R_h\right)^{-1}+4.92438\cdot\left(R_h\right)^{-0.768}-0.89002\cdot\left(R_h\right)^{-0.536}+0.05507\cdot\left(R_h\right)^{-0.304}} \tag{2}$$

In order to determine the return period (in years) linked to the probability of occurrence of two simultaneous WDR_{zi} and $DRWP_{zi}$ exposures, an innovative approach to the Bayes' Theorem was implemented. Since $DRWP_z$ is solely dependent on the variable U_{10} (see Eq. 1), the occurrence probability of a specific $DRWP_{zi}$ value can be substituted by that of the corresponding U_{10i} value (Eq. 3). In turn, the probability of a WDR_{zi} value when the prior simultaneous wind speed U_{10i} is occurring, can be expressed as the occurrence probability of the R_{hi} value that can be solved through Eq. 2.

Therefore, the BPB method simplifies the mathematical issue into a straightforward probability calculation of two independent variables (U_{10i} and R_{hi} values obtained from Eqs, 1 and 2, respectively).

$$\frac{1}{\text{Return period}\ \left(WDR_{Z\,i} \cap DRWP_{Z\,i}\right)} = P\left(WDR_{z\,i} \cap DRWP_{z\,i}\right) = P\left(DRWP_{Z\,i}\right) \cdot P\left(WDR_{z\,i} \mid DRWP_{z\,i}\right) = P\left(U_{10i}\right) \cdot P\left(R_{hi}\right) \quad (3)$$

To functionally calculate both independent probabilities, a Gumbel distribution (extreme value analysis) is recommended [14, 21]. These probabilities $P(U_{10i})$ and $P(R_{hi})$ are determined by statistically analysing series of annual maxima of U_{10} and R_h records, being $u_{(u10)}$ and $u_{(Rh)}$ the mode of both series and $\beta_{(u10)}$ and $\beta_{(Rh)}$ the dispersion parameter, respectively. As a result, Eq. 4 completes a three-equation system that enables determining the return period associated with the occurrence of specific WDR_{zi} and $DRWP_{zi}$ exposures on any building façade. By knowing the façade location and features (i.e. $u_{(u10)}$, $u_{(Rh)}$, $\beta_{(u10)}$, $\beta_{(Rh)}$, z, and z_o values), this equation system (Eqs. 1, 2 and 4) can be analytically solved by fixing two of the five unknowns: WDR_{zi}, $DRWP_{zi}$, Return period, U_{10i} and R_{hi} (Figure 1).

$$\frac{1}{\text{Return period}\ \left(WDR_{Zi} \cap DRWP_{Zi}\right)} \approx \left(1 - \exp^{-\exp^{-\left(U_{10i} - u(U_{10})\right)/\beta(U_{10})}}\right) \cdot \left(1 - \exp^{-\exp^{-\left(R_{hi} - u(R_h)\right)/\beta(R_h)}}\right) \quad (4)$$

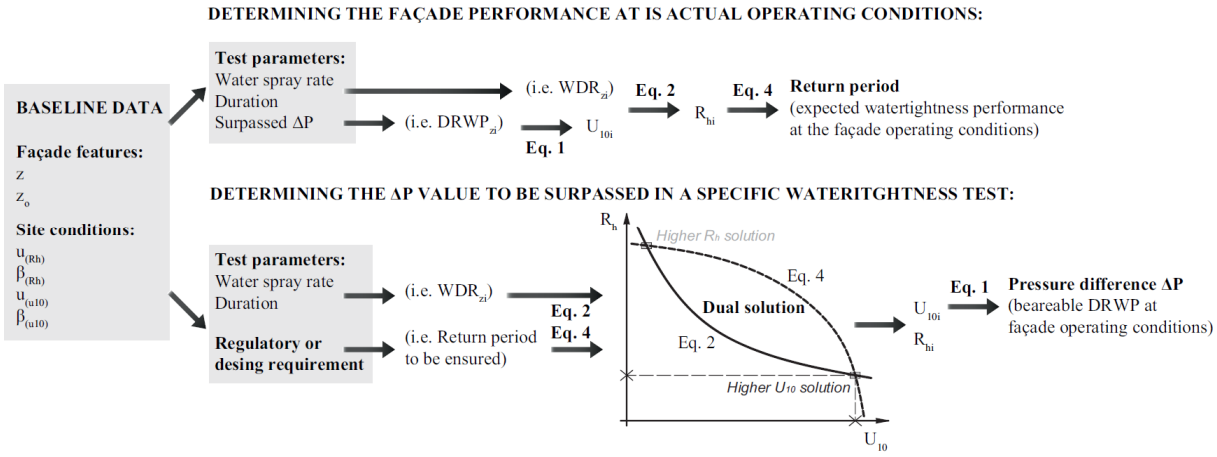

Figure 1: Scheme of the BPB method implementation.

On the one hand, the product of the water spray rate ($l/m^2 \cdot min$) used in testing by the test duration can be taken as WDR_{zi} (l/m^2) and the pressure difference ΔP (Pa) overcome by the façade sample as $DRWP_{zi}$. Thus, the U_{10i} and R_{hi} values and the return period associated with this blended exposure tested can be determined. This approach allows for quantifying the performance of the façade configuration under its actual use conditions, expressed as the return period linked to the maximum exposures it can withstand.

Alternatively, U_{10i} and R_{hi} values can be solved based on the water spray rate and duration established in the test (WDR_{zi} value) and setting a target Return period of watertightness set according to regulatory requirements and design decisions. This approach allows to obtain the pressure difference ΔP ($DRWP_{zi}$ value) that must be surpassed during the test to recreate the specified return period. Setting other pairs of unknowns makes no physical sense, as U_{10i} and R_{hi} are intermediate variables and the duration and water spray rate (WDR_{zi}) are constants predetermined for each watertightness test.

2.1. Comprehensive and functional implementation proposed for the BPB method

However, there are still methodological challenges in this equation that limit its applicability and reliability:

Firstly, the recording interval used in Eq. 4 (associated with $u_{(u10)}$, $u_{(Rh)}$, $\beta_{(u10)}$, and $\beta_{(Rh)}$ values) is defined by the weather records available at each location (e.g., hourly or daily), whereas the U_{10i} and R_{hi} values solved in Eqs. 1 and 2 are linked to the duration of the watertightness tests (differential pressure stages usually range from 5 to 15 minutes) [10-11]. When the test duration does not align qwith the available recording interval, an intermediate calculation is requited to extrapolate the U_{10i} and R_{hi} values to their equivalents in the required recording interval for Eq. 4.

In addition, the site-specific $u_{(u10)}$ and $\beta_{(u10)}$ values (used in Eq. 4) are usually based on maximum annual records that do not account for co-occurrence with precipitation. Consequently, both values may not be suitable for calculating the recurrence of wind speed values concurrent with rainfall as determined in Eq. 1. Thus, a prior re-analysis of wind speed records must be also addressed.

To deal with the first methodological issue, recent research has identified general forms of regressions that effectively extrapolate extreme values of rainfall intensity (mm/min) and wind speed (m/s) across different subdaily recording intervals [22]. For rainfall intensity, a regression of potential type was identified to accurately relate the maximum annual values associated with different subdaily intervals (Eq. 5). $R_{h(t)}$ (mm/min) represents the rainfall intensity associated with any t-minute recording interval during extreme precipitation events, and the empirical coefficients a and b are site-specific. Similarly, a logarithmic regression has been found to be the most suitable for relating the maximum annual wind speeds associated with different subdaily intervals (Eq. 6). In this case, $U_{10(t)}$ (m/s) represents the wind speed associated with a t-minute record of extreme wind events, while the empirical coefficients c and d also vary according to the location.

$$R_{h\,(t)} = a \cdot t^{-b} \tag{5}$$

$$U_{10(t)} = -c \cdot \ln(t) + d \tag{6}$$

Both Eqs. 5 and 6 can be included into the BPB method to extrapolate, by a cross-multiplication, the resolved U_{10i} and R_{hi} values to any recording interval required by Eq. 4. In practice, the regressions specific to each site (coefficients a, b, c and d) could be identified based on weather records belonging to only two subdaily recording intervals by conducting a least-squares regression analysis (LSRA) on the average of maximum annual values associated with both recording intervals (e.g. hourly and daily records, to mention the most common). Typical spreadsheets can be used for this calculation.

However, the available annual maxima of wind speed generally do not differentiate concurrence with rainfall, which could affect the reliability of the logarithmic regression when applied in the BPB method. This is also linked to the second challenge mentioned above. To address this issue, the available series of wind speed records should be screened to exclude those wind data non-concurrent with rainfall. The resulting series will provide maximum annual values of wind speed simultaneous to rainfall for each recording interval, and these maxima can be averaged to obtain a single representative value per recording interval. This reanalysis offers several methodological improvements:

The mode and dispersion parameters required to solve Eq. 4 can be calculated based on these re-elaborated series of wind speed extremes simultaneous to rainfall ($U_{10\ sim}$). Thus, specific $u_{(u10\ sim)}$ and $\beta_{(u10\ sim)}$ values can be identified for each recording interval and location. Both values can then be used to calculate return periods that really represents the recurrence of WDR events.

Moreover, preliminary findings obtained in The Netherlands suggest that the annual maxima of wind speed concurrent with rainfall can be equally related using the same logarithmic regression presented in Eq. 6. Thus, a LRSA can also be applied to determine improved coefficients c_{sim} and d_{sim} for Eq. 6, specifically tailored to relate extreme wind speeds concurrent with rainfall (such as those solved in Eq. 1) across different recording intervals.

3. IMPLEMENTATION EXAMPLES AND DISCUSSION

To illustrate these improvements in the implementation of the BPB method, this work considered simultaneous climatic records gathered from two Spanish cities over a 10-year period. Both locations are characterised by different climates: temperate oceanic climate in Pontevedra and hot-summer Mediterranean climate in Málaga. In turn, two hypothetical façades with differentiated features are analysed applying both resolution options (the façade features are summarised in Table 1). In the case of Pontevedra, 10-minute records of rainfall and wind speed, along with wind gust records (3-second interval), were available. For Malaga, only 30' agroclimatic records referred to a height of 2 m were available. All data were collected by official organisations following the guidelines set by the World Meteorological Organization (WMO) [23-25]. Throughout the years considered, only 0.009% and 0.095% of missing data were identified in Pontevedra and Malaga, respectively.

Table 1: Summary of the calculation parameters applicable in the two cities and the features of the two façades analysed (height and surroundings).

PONTEVEDRA (Lourizan station)										
Altitude (m)		**Longitude (DD)**		**Latitude (DD)**		**Average rainfall (mm/yr)**			**Avg. wind speed (m/s)**	
57.0		-08.664220		42.409200		1,514			1.3	
Façade features:										
Height (m):	9.0	**Roughness length z_0 (m):**		1.5 (city outskirts) [15]						
Site conditions:										
Maximum rainfall intensity (mm/min); Average of maximum annual records for each recording interval:										
	10'	**20'**	**30'**	**40'**	**1 h**	**360'**	**480'**	**720'**	**1 day**	**Eq. 5** (by LSRA)
	1.064	0.640	0.505	0.404	0.326	0.114	0.092	0.072	0.047	$R_{h\,(t)} = 4.138 \cdot t^{-0.617}$
				$u_{(Rh)}$:	14.754					*(R^2 = 0.9991)*
				$\beta_{(Rh)}$:	9.645					
Maximum wind speed CONCURRENT with rainfall (m/s); Average of annual maxima records for each recording interval:										
gust	**10'**	**20'**	**30'**	**40'**	**1 h**	**360'**	**480'**	**720'**	**1 day**	**Eq. 6** (by LSRA)
21.746	9.824	9.068	8.212	7.517	7.098	5.223	4.642	4.015	3.091	$U_{10(t)} = -1.765 \cdot \ln(t) + 14.997$
				$u_{(u10\ sim)}$:	6.265					*(R^2 = 0.9696)*
				$\beta_{(u10\ sim)}$:	1.682					

MÁLAGA										
Altitude (m)		**Longitude (DD)**		**Latitude (DD)**		**Average rainfall (mm/yr)**			**Avg. wind speed (m/s)**	
57.0		-04.536391		36.757833		368			1.4	
Façade features:										
Height (m):	36.0	**Roughness length z_0 (m):**		3.0 (downtown city area with high rise buildings) [15]						
Site conditions:										
Maximum rainfall intensity (mm/min); Average of maximum annual records for each recording interval:										
			30'		**1 h**	**360'**	**480'**	**720'**	**1 day**	**Eq. 5** (by LSRA)
			0.677		0.425	0.253	0.158	0.123	0.095	$R_{h\,(t)} = 7.933 \cdot t^{-0.716}$
				$u_{(Rh)}$:	14.754					*(R^2 = 0.9986)*
				$\beta_{(Rh)}$:	9.645					
Maximum wind speed CONCURRENT with rainfall (m/s); Average of annual maxima records for each recording interval:										
			30'		**1 h**	**360'**	**480'**	**720'**	**1 day**	**Eq. 6** (by LSRA)
			5.272		4.479	3.734	2.848	2.197	2.125	$U_{10(t)} = -1.127 \cdot \ln(t) + 9.0131$
				$u_{(u10\ sim)}$:	4.016					*(R^2 = 0.9867)*
				$\beta_{(u10\ sim)}$:	0.935					

Additional data series of rainfall and wind speed, corresponding to other recording intervals, were produced by applying the aggregation and average procedures set by the WMO to the available records [23]. Additionally, the wind speed data were re-analysed by excluding non-concurrent records with precipitation. This allows for determining the annual maxima of both variables for different recording intervals and subsequently identifying representative values per variable, recording interval, and location. Thus, the potential and logarithmic regressions that best relate these averages (Eqs. 5 and 6) can be identified by means of a LSRA, determining the most suitable coefficients a, b, c_{sim}, and d_{sim} for each location. The calculation parameters associated with both locations (site conditions) are also summarised in Table 1.

3.1. Characterising the façade performance at its use conditions

In the case of Pontevedra, it is intended to quantify the watertightness performance of a building façade of 9 m height, located at the city outskirts. For the purpose of analysis, it is assumed that the façade configuration withstood a pressure difference ΔP of 300 Pa during the EN 12865 watertightness test. This test is characterised by pressure stages of 10 minutes and a water spray rate of 2 l/m^2·min [10]. To determine the watertightness performance of the façade, the wind speed required to generate a DRWP exposure of 300 Pa on the analysed façade can be obtained by solving Eq. 1.

$$300\ \text{Pa} = 1 \cdot \frac{1}{2} \cdot 1.2 \cdot \left(U_{10(10\ \text{min})}\right)^2 \cdot \left(\frac{9}{10}\right)^{2 \cdot \left[0.18+0.13 \cdot \log 1.5+0.03 \cdot (\log 1.5)^2\right]} \cdot 1 \quad \Rightarrow \quad U_{10(10\ \text{min})} = 22.846\ \text{m/s}$$

In turn, the rainfall intensity required to result in 20 mm of WDR on this façade (2 l/m^2·min applied over 10 min), while there is a concurrent wind speed of 22.846 m/s, can be obtained using Eq. 2:

$$20\ mm = 1.14 \cdot 0.9 \cdot \frac{22.846 \cdot \left(\frac{9}{10}\right)^{\left[0.18+0.13 \cdot \log 1.5+0.03 \cdot (\log 1.5)^2\right]}}{-0.16603 \cdot \left(R_{h(10\ \text{min})}\right)^{-1} + 4.92438 \cdot \left(R_{h(10\ \text{min})}\right)^{-0.768} - 0.89002 \cdot \left(R_{h(10\ \text{min})}\right)^{-0.536} + 0.05507 \cdot \left(R_{h(10\ \text{min})}\right)^{-0.304}}$$

$$R_{h\ (10\ \text{min})} = 4.522\ \text{mm} = 0.452\ \text{mm/min}$$

In order to substitute both 10-minute values in Eq. 4 (where the considered u and β values only refer to the hourly recording interval available at the location), a cross-multiplication based on Eqs. 5 and 6 needs to be applied beforehand. Thus, the equivalent hourly values can be determined as follows:

$$R_{h\ (60\ \text{min})} = R_{h(10\ \text{min})} \cdot \frac{4.138 \cdot 60^{-0.617}}{4.138 \cdot 10^{-0.617}} = 0.150\ \text{mm/min} = 8.98\ \text{mm}$$

$$U_{10(60\ \text{min})} = U_{10(10\ \text{min})} \cdot \frac{-1.765 \cdot \ln(60) + 14.997}{-1.765 \cdot \ln(10) + 14.997} = 16.238\ \text{m/s}$$

These equivalent hourly values can be directly substituted into Eq. 4 to calculate the return period associated with the maximum exposure that this façade configuration would withstand under its design operating conditions. Based on the result, it would be reasonable to consider a façade configuration with a lower watertightness performance to prevent bloated designs against rainwater penetration.

$$\frac{1}{\text{Return period}\ (20\ \text{mm} \cap 300\ \text{Pa})} = \left(1 - \exp^{-\exp^{-(16.238\ -\ 6.265)/1.682}}\right) \cdot \left(1 - \exp^{-\exp^{-(8.98\ -\ 14.754)/9.645}}\right)$$

$$\text{Return period}\ (20\ \text{mm} \cap 300\ \text{Pa}) = 449.1\ \text{years}$$

3.2. 3.2 Determining the pressure difference to overcome in a particular watertightness test

In the case of Málaga, it is intended to design a 36 m high curtain wall in the city centre, which can ensure watertightness for at least 100 years. For this, the pressure difference ΔP to overcame during the EN 12155 test (5-minute pressure stages and a water spray rate of 2 l/m^2·min) will be determined [11]. This involves solving the two-equation system defined by Eqs. 2 and 4, where the unknowns U_{10i} and R_{hi} can be found. Before that, the cross-multiplication that allows extrapolating the hourly values equivalent to those linked with the 5-minute duration of the watertightness test should be applied.

$$R_{h\,(60\ \mathrm{min})} = R_{h\,(5\ \mathrm{min})} \cdot \frac{7.933 \cdot 60^{-0.716}}{7.933 \cdot 5^{-0.716}} = 0.169 \cdot R_{h\,(5\ \mathrm{min})} \qquad U_{10(60\ \mathrm{min})} = U_{10(5\ \mathrm{min})} \cdot \frac{-1.127 \cdot \ln(60) + 9.0131}{-1.127 \cdot \ln(5) + 9.0131} = 0.611 \cdot U_{10(5\ \mathrm{min})}$$

$$10\ mm = 1.14 \cdot 0.9 \cdot \frac{U_{10i(5\ \mathrm{min})} \cdot \left(\frac{36}{2}\right)^{\left[0.18+0.13 \cdot \log 3.0+0.03 \cdot (\log 3.0)^2\right]}}{-0.16603 \cdot \left(R_{h(5\ \mathrm{min})}\right)^{-1} + 4.92438 \cdot \left(R_{h(5\ \mathrm{min})}\right)^{-0.768} - 0.89002 \cdot \left(R_{h(5\ \mathrm{min})}\right)^{-0.536} + 0.05507 \cdot \left(R_{h(5\ \mathrm{min})}\right)^{-0.304}}$$

$$\frac{1}{100\ \mathrm{years}} = \left(1 - \exp^{-\exp^{-\left(0.611 \cdot U_{10i(5\ \mathrm{min})} - 4.016\right)/0.935}}\right) \cdot \left(1 - \exp^{-\exp^{-\left(0.169 \cdot R_{hi(5\ \mathrm{min})} \cdot 60 - 14.754\right)/9.645}}\right)$$

$$U_{10(5\ \mathrm{min})} = 13.553\ \mathrm{m/s} \qquad R_{h\,(5\ \mathrm{min})} = 0.327\ \mathrm{mm} = 1.635\ \mathrm{mm/min}$$

As shown in Figure 1, this two-equation system also yields an alternative solution ($R_{hi\,(5min)}$ = 5.838 mm and $U_{10i\,(5\ min)}$ = 1.315 m/s), which has no interest since it provides a lower wind speed (the pressure difference is the key factor in all the watertightness tests). Lastly, the obtained wind speed enables the calculation of the pressure difference to be overcome in this watertightness test (Eq. 1):

$$DRWP = \Delta P = 1 \cdot \frac{1}{2} \cdot 1.2 \cdot \left(U_{10(5\ \mathrm{min})}\right)^2 \cdot \left(\frac{36}{2}\right)^{2 \cdot \left[0.18+0.13 \cdot \log 3.0+0.03 \cdot (\log 3.0)^2\right]} \cdot 1 = 464\ \mathrm{Pa}$$

This comprehensive implementation of the method can equally be conducted using limited weather records (e.g. hourly and daily data), without the need to generate additional data series as was done in the analysed case studies.

4. CONCLUSIONS

It has been shown how it is possible to resolve the methodological weaknesses affecting the reliability and functionality of the BPB method by considering only wind speed records concurrent with rainfall. Through the proposed re-analysis, the BPB method offers an accurate and comprehensive assessment of the watertightness performance of building façades against rainwater penetration. It also allows for the quantitative estimation of the required pressure difference to withstand in any international watertightness test to meet specific design requirements. These improvements have been applied in two case studies characterised by different climates and façade features. The effective implementation of this performance-based design tool throughout Spain is planned as part of the HUEFAES research project PID2021-122203OB-I00, producing a complete database of calculation parameters related to multiple Spanish locations.

5. ACKNOWLEDGEMENTS

Project *PID2021-122203OB-I00* funded by MCIN/AEI/10.13039/501100011033 and by ERDF A way of making Europe.

6. BIBLIOGRAPHY

[1] Bastien D, Winther-Gaasvig M. Influence of driving rain and vapour diffusion on the hygrothermal performance of a hygroscopic and permeable building envelope. *Energy*. 2018; 164:288–297. https://doi.org/10.1016/j.energy.2018.07.195.

[2] Mendell MJ, Mirer AG, Cheung K, Tong M, Douwes J. Respiratory and allergic health effects of dampness, mold, and dampness-related agents: A review of the epidemiologic evidence. *Environ Health Perspect*. 2011; 119:748-756. https://doi.org/ 10.1289/ehp.1002410.

[3] Orr SA, Cassar M. Exposure indices of extreme wind-driven rain events for built heritage. *Atmosphere-Basel* 2020; 11:163. https://doi.org/10.3390/atmos11020163.

[4] Blocken B, Derome J, Carmeliet J. Rainwater runoff from building façades: a review. *Build Environ*. 2013; 60:339–361. https://doi.org/10.1016/j. buildenv.2012.10.008.

[5] Galbraith GH, McLean RC, Kelly D. Moisture permeability measurements under varying barometric pressure. *Build Res Inf*. 1997; 25:348–353. https://doi.org/10.1080/096132197370165.

[6] Blocken B, Carmeliet J. A review of wind-driven rain research in building science. *Build Environ*. 2004; 92(13):1079-1130. https://doi.org/10.1016/j.jweia.2004.06.003.

[7] CEN. EN ISO 15927-3, Hygrothermal performance of buildings - Calculation and presentation of climatic data Part 3: Calculation of a driving rain index for vertical surfaces from hourly wind and rain data. Brussels, Belgium: European Committee for Standardization; 2009.

[8] Pérez JM, Domínguez J, del Coz JJ, Martínez JE. Directional characterisation of annual and temporary exposure to rainwater penetration on building façades throughout Mexico, *Build Environ*. 2022; 2012:108837. https://doi.org/10.1016/j.buildenv.2022.108837.

[9] Domínguez J, Pérez JM, Alonso M, Cano E, del Coz JJ. Assessment of water penetration risk in building façades throughout Brazil. *Build Res Inf*. 2015; 45(5):1–16. https://doi.org/10.1080/09613218.2016.1183441.

[10] CEN. EN ISO 12865, Hygrothermal performance of building components and building elements - Determination of the resistance of external wall systems to driving rain under pulsating air pressure. Brussels, Belgium: European Committee for Standardization; 2001.

[11] CEN. EN 12155, Curtain walling - Watertightness - Laboratory test under static pressure. Brussels, Belgium: European Committee for Standardization; 2000.

[12] Pérez JM, Domínguez J, Rodríguez B, del Coz JJ, Cano E. A new method for determining the water tightness of building facades. *Build Res Inf*. 2013; 41(4):401–414. https://doi.org/10.1080/09613218.2012.774936.

[13] Pérez JM, Domínguez J, Rodríguez B, del Coz JJ, Cano E, Navarro A. An extended method for comparing watertightness tests for facades. *Build Res Inf*. 2013; 41(6):706–721. https://doi.org/10.1080/09613218.2013.823538.

[14] Pérez JM, Domínguez J, Rodríguez B, Cano E, del Coz JJ, Álvarez FP. Improvement alternatives for determining the watertightness performance of building facades. *Build Res Inf*. 2015; 43(6):723-736. https://doi.org/ 10.1080/09613218.2014.943101.28.

[15] Bañuelos F, Ángeles C, Ríos S. Analysis and validation of the methodology used in the extrapolation of wind speed data at different heights. *Renew Sust Energ Rev*. 2010; 14:2383-2391. https://doi.org/10.1016/j.rser.2010.05.001.

[16] Smedman-Högström AS, Högström U. A practical method for determining wind frequency distributions for the lowest 200 m from routine meteorological data. *J Appl Meteorol*. 1978; 17:942-954. https://doi.org/0021-8952/0942-0954$06.50.

[17] Gualteri G, Secci S. Comparing methods to calculate atmospheric stability-dependent wind speed profiles: A case study on coastal location. *Renew Energ*. 2011; 36:2189-2204. https://doi.org/10.1016/j.renene.2011.01.023.

[18] Straube JF, Burnett EFP. In: Wisse J, Hendriks N, Schellen H, van de Spoel W, eds. Simplified prediction of driving rain on buildings. Proceedings International Building Physics Conference, Eindhoven; September 18-21, 2000:375–382.

[19] Van der Bossche N, Lacasse MA, Janssens A. A uniform methodology to establish test parameters for watertightness testing. Part I: Pareto front analysis on co-occurring rain and wind. *Build Environ*. 2013; 63:157-167. ttps://doi.org/10.1016/j.buildenv.2012.12.019.

[20] Cornick SM, Dalgliesh A, Said N, Djebbar R, Tariku F, Kumaran MK. Report from Task 4 of MEWS Project: Task 4 – Environmental conditions final report (Research Report No. 113). Ottawa, Canada: National Research Council Canada; 2002.

[21] Gumbel EJ. Statistics of extremes. New York, USA: Columbia University Press; 1958.

[21] Pérez JM, Domínguez J, Martínez JE, Alonso M, del Coz JJ. An alternative approach to estimate any subdaily extreme of rainfall and wind from usually available records. *Stoch Environ Res Risk Assess*. 2022; 36:1819–1833. https://doi.org/10.1007/s00477-021-02144-4.

[23] WMO. Guide to meteorological instruments and methods of observation (WMO No. 8). Geneve, Switzerland: World Meteorological Organisation; 2008.

[24] Xunta of Galicia. *Observation. Weather reports. Data access*. S*tation list*. https://www.meteogalicia.gal/observacion/rede/redeIndex.action (accessed: June 2023)

[25] Junta of Andalusia. *Andalusian agroclimatic information network.* https://www.juntadeandalucia.es/agriculturaypesca/ifapa/riaweb/web/estacion/29/1 (accessed: June 2023)